

# Effect of Organo-Phosphorus and Nano-Clay Materials on the Thermal and Fire Performance of Epoxy Resins

M. Hussain,<sup>1</sup> R. J. Varley,<sup>2</sup> Z. Mathys,<sup>3</sup> Y. B. Cheng,<sup>1</sup> G. P. Simon<sup>1</sup>

<sup>1</sup>*School of Physics and Materials Engineering, Monash University, Clayton, Vic-3180, Australia*

<sup>2</sup>*CSIRO Molecular Science, Clayton, Vic-3168, Australia*

<sup>3</sup>*DSTO, Platforms Science Laboratory, P.O. Box 4331, Melbourne 3001, Australia*

Received 24 January 2003; accepted 13 May 2003

**ABSTRACT:** The results of flame retardance and thermal stability of a reactively modified organo-phosphorus diglycidylether of bisphenol-A and an organo-phosphorus tetraglycidyl diaminodiphenylmethane are reported here. The organo-phosphorus epoxy resins were synthesized by the reaction of 9,10-dihydro-9-oxa-10-phosphaphenanthrene-10-oxide and diglycidyl ether of bisphenol-A and tetraglycidyl diaminodiphenylmethane, respectively, and then cured with a mixture of 3,5-diethyltoluene-2,4-diamine and 3,5-diethyltoluene-2,6-diamine. In addition to this, between 5 and 7.5% of organically modified polymeric layered silicate nano-clay was also added to neat epoxy resin or to the phosphorus-modified epoxy resin to investigate any synergies, or otherwise, a combination of clay and phosphorus on the flame, degradation, and thermal properties are also re-

ported. The reaction kinetics of phosphorus-modified and epoxy cure were studied by FTIR, <sup>1</sup>H-NMR, and DSC. Thermal properties and morphology of the final product were analyzed by thermogravimetric analysis, dynamic mechanical thermal analysis, X-ray diffraction, and cone calorimetry. Improvement in flame retardance by cone calorimetry was demonstrated by the addition of only 3% phosphorus or 7.5% clay into the epoxy compared with unmodified epoxy resins, whereas no evidence of synergy for a phosphorus and clay combination was found. © 2003 Wiley Periodicals, Inc. *J Appl Polym Sci* 91: 1233–1253, 2004

**Key words:** resins; thermal properties; clay; nanocomposites; kinetics (polym.)

## INTRODUCTION

Epoxy resins are widely used in many industrial applications such as coatings, adhesives, electronic devices, automobiles, marine vessels, and space vehicles because of their low manufacturing cost, ease of processing, low shrinkage, good chemical and electrical resistance, and good mechanical properties.<sup>1–5</sup> However, because of their inherently brittle nature, additives and modifiers are generally used to improve their physical and mechanical properties. In particular, it is becoming increasingly important, based on more stringent regulatory requirements, for the fire worthiness of epoxy resins to be substantially improved. Halogen-containing compounds are commonly applied as flame retardants in epoxy resins, either by blending or chemical modification to improve their thermal and flame-retardant properties, but because of their toxic gas emissions are becoming much less favored. Various fillers such as antimony trioxide, magnesium hydroxide, silicon, and boron-based compounds are also often used with considerable effect but tend to require such high levels of

addition that processability and final properties can be compromised. In general the addition of these types of fillers to epoxy resins can significantly influence their combustion behavior, by increasing ignition time and decreasing heat release rate, but can also increase the amount of toxic and corrosive fumes during thermal decomposition, making their further usage limited.

In recent times, phosphorus compounds have been used as effective fire retardants, usually as additives and more recently by being incorporated into the backbone of the epoxy resin or the amine hardeners. The advantage of being covalently linked into the backbone of chemical species of epoxy is that far fewer phosphorus species are required to increase the effectiveness as a fire retardant. A variety of chemical approaches have been used by many investigators.<sup>6–12</sup> Examples of this strategy of incorporating a phosphorus species into the structure of the network reported in the literature are as follows. Buckingham et al. synthesized phosphorylated flame-retardant curatives for epoxy resins,<sup>13</sup> whereas Chiu et al. modified the epoxy resin diglycidylether of bisphenol-A (DGEBA) with diphenylphosphonic chloride and polymerizing the system with diethyltrianmine (DETA).<sup>14</sup> Recently Shu et al. modified DGEBA by the imidization of bis(3-aminophenyl)phenylphosphine oxide (BMIPO) to produce phosphorus-containing epoxy.<sup>15</sup> Wang et al. also synthesized phosphorus-containing DGEBA-type epoxide and showed that the thermal properties

Correspondence to: M. Hussain.

can be improved.<sup>16</sup> In a previous study, this laboratory synthesized a phosphorus-containing DGEBA, polymerized with a commercial diethyl toluene diamine hardener and which showed that the flame retardance and thermal stability were improved by attaching a phosphorus group to a small proportion of epoxy units.<sup>17</sup> It was found that the amount of phosphorus content increases the char yield and the limiting oxygen index (LOI) value. In that previous study<sup>17</sup> and in the work reported here, a bifunctional DGEBA resin was used, as is the case in all previous reports in this area. However, in the aerospace industry, for example, resins of greater functionality and glass transition are usually used, such as in high performance carbon-fiber prepregs. Very few investigations have been reported for the most widely used tetrafunctional epoxies, tetraglycidyl diamino phenyl amine (TGDDM). In this work DGEBA and TGDDM were modified with a phosphorus-containing compound with the aim of improving its flame retardance. To the best of our knowledge for the first time a tetrafunctional epoxy resin system has been modified with a phosphorus group to use in a high-performance application.

In addition to this, the ability of polymer-clay nanocomposites<sup>18,19</sup> to improve flame retardance has been studied in very recent work (only in DGEBA resin system). Gilman and collaborators studied the flammability of polymer/layer-inorganic composites, with the emphasis on polymer/montmorillonite and polymer/fluorohectorite hybrids.<sup>20-23</sup> They showed that the use of exfoliated montmorillonite clay in polyamide-6 clay nanocomposites leads to promising flame-retardant performance. Several other polymer systems were also investigated using cone calorimetry studies, including bisphenol-based epoxides, vinyl esters, and polystyrene.<sup>21-23</sup> Evidence was found for a common mechanism on thermal stability and flammability reduction and it was found that addition of nano-clays can substantially aid flame retardance by encouraging the formation of a strong char, which limits the passage of degradation products from the matrix that in turn lead to continued fueling of the fire. However, it is usually found that such clay additions are not themselves sufficiently effective to be classified as flame retardants. It is also possible that the combination of inorganic materials (such as nano-clay) in combination with other forms of flame retardant additive may be more effective. This has not been reported yet and is an important focus of this work.

In this study we set out to improve the flame retardance of both DGEBA and TGDDM epoxy resins in a number of ways: by incorporation of phosphorus alone, by addition of layered silicate nano-clays, and by the combination of both nano-clays and phosphorus. The intention was to determine whether the combination of both additives in clay and phosphorus modification displays a synergistic effect in terms of

fire performance. Such a combination may also have advantages in terms of thermal properties and thus a wide range of techniques was used to characterize the properties of the system: both by thermogravimetry, which is often reported in epoxy fire-retardant work, and by cone calorimetry using an oxygen calorimeter that satisfactorily simulates the fire properties of polymers.

## EXPERIMENTAL

### Materials

The epoxy resins used in the study were the diglycidyl ether of bisphenol-A (DGEBA), commercially known as DER-331 (Dow Chemical Company, Australia) and tetrafunctional tetraglycidyl diamino diphenylmethane (TGDDM), commercially known as Araldite MY 720 (Vantico, Australia). The organo-phosphorus compound 9,10-dihydro-9-oxa-10-phosphaphenanthrene-10-oxide (DOPO) was obtained from Tokyo Kasei Kogyo Co. (Japan). The amine curing agent used in this experiment was the aromatic isomer mixture of 3,5-diethyltoluene-2,4-diamine and 3,5-diethyltoluene-2,6-diamine (DETDA), commercially known as Ethacure-100 (Albemarle Corp.), which is widely used in high-performance epoxy resin systems. Octadecyl ammonium ion-exchanged modified montmorillonite layered silicate clay, commercially known as Nanomer 1.30E, with an initial interlayer *d*-space of 23 Å, was also used in this study. Table I shows the chemical structure of epoxy resins, DOPO, and the curing agent used in this work. All of the materials were used as received, without any further purification.

### Synthesis of organo-phosphorus epoxy resins

DGEBA or TGDDM epoxy resin (250 g) was charged into a three-neck round-bottom flask and heated to 130°C in an oil bath connected to a temperature controller. DOPO (66 g) was added and mixed with a mechanical stirrer at 500 rpm, maintaining the temperature at 130°C until a clear solution was obtained.<sup>24</sup> The temperature was then raised to 180°C and stirring continued for a further 5 h until a transparent solution of 3% phosphorus-DGEBA/TGDDM epoxy was obtained. The epoxy final equivalent weight was determined following the method described elsewhere.<sup>25</sup>

### Preparation of epoxy-clay nanocomposites

Clay was dried for 24 h at 50°C under vacuum before sample preparation. The layered clay was then dispersed in the virgin resin at 80°C using the stirrer at 50 rpm. After mixing clay and resin for 30 min, the curing agent was added and mixed in a rotary evaporator under vacuum for 1-2 h for degassing at 70°C. To fabricate phosphorus-containing epoxy nanocompos-

TABLE I  
Epoxy Resins, Hardener, and Organophosphorous Compound Used in This Experiment

Material	Formula
DGEBA	
TGDDM	
DOPO	
DETDA	

ites, the desired amount of clay was added to the phosphorus-modified epoxy resins and stirred for 1 h before addition of amine curing agent and subsequent stirring. After mixing in the clay for 30 min, the curing agent was added and mixed in a rotary evaporator under vacuum for 1–2 h to allow degassing at 70°C. The catalyzed mixtures were poured into Teflon-coated molds and cured for 6 h at 120°C followed by postcure for 2 h at 200°C. The cured samples were then cut to the desired sample size for mechanical and fire-resistance testing.

### Methods

<sup>1</sup>H-NMR spectra of DGEBA or TGDDM, DOPO, and reaction of DGEBA/TGDDM–DOPO at 130 and 200°C were recorded with a Bruker 500-MHz <sup>1</sup>H-NMR spectrometer (Bruker Instruments, Billerica, MA). Fourier transform infrared (FTIR) was observed on a Perkin–Elmer FTIR spectrometer (Perkin Elmer Cetus Instruments, Norwalk, CT). Wavenumbers were recorded from 400 to 4000 cm<sup>-1</sup> for mid infrared and 4000–8000 cm<sup>-1</sup> for near infrared. Wide-angle X-ray diffraction

(XRD) analyses to determine the degree of clay delamination were performed on a Rigaku Geigerflex generator (Rigaku, Tokyo, Japan) with a wide-angle goniometer. An acceleration voltage of 40 kV and current of 22.5 mA were applied using Ni-filtered Cu–K<sub>α</sub> radiation.

To observe the interlayer distance of the clay, and to understand the dispersion behavior of clays in the epoxy matrix, transmission electron microscopy (TEM) was used. The samples were prepared using a Porter-Blum MT-2B ultramicrotome with a DiaTech diamond knife. Cuts were made at an angle of 6°, and cutting velocity was kept at 0.1 mm/s. Samples were collected on hexagonal 300-mesh copper grids. Micrographs were then taken from a Philips transmission electron microscope (Philips, The Netherlands) at 200 kV in the bright-field mode.

The epoxy resins DGEBA/TGDDM, 3% phosphorus–DGEBA/TGDDM, 7.5% clay–DGEBA/TGDDM, and 3% phosphorus–7.5% clay–DGEBA/TGDDM were mixed with curing agent DETDA, in a stoichiometric ratio. The heat of mixture released during the cure was measured by DSC on a Perkin–Elmer DSC-7

in a nitrogen atmosphere. The DSC was calibrated with indium and zinc standards. Samples of 7–10 mg were sealed in aluminum pans and heated from 50 to 300°C at a scanning rate of 10 K/min.

Thermogravimetric analysis was performed on the cured samples using a TG-92 Setaram thermal analyzer. The thermographs were obtained at a heating rate of 10°C/min using 10–15 g of the powdered sample. The experiments were made in a flowing air atmosphere. The loss tangent spectrum ( $\tan \delta$ ) of cured samples was determined using a DMTA IV dynamic mechanical thermal analyzer (Rheometrics Scientific, Amherst, MA). The cured samples were clamped in a medium frame using a small center clamp in the dual-cantilever mode. Scans were performed from 80 to 260°C at 2°C/min at a frequency 1 Hz. The main data abstracted from these runs were the glass-transition temperatures corresponding to the temperature location of the maximum value of  $\tan \delta$ .

Cone calorimetry was used to investigate the combustion behavior under ventilated conditions including time to ignition (TTI), rate of heat release (RHR), time to reach maximum (RHR), smoke density, carbon monoxide, and carbon dioxide evolution; samples of mass loss were determined by cone calorimetry in accordance with the procedure described in an ASTM standard method.<sup>26</sup> The heat flux used was 50 kW/m<sup>2</sup> on the specimen, which had an exposed surface of 100 × 100 × 4 mm. The device consisted of a radiant electric heater in a trunk-conic shape, an exhaust gas system with oxygen monitoring and instrument to measure the gas flux, an electric spark for ignition, and a load cell to measure the weight loss. All tests were terminated after 500 s of exposure. TTI measures the time to achieve sustained flaming combustion at a particular cone irradiance. Smoke density was measured by the decrease in transmitted light intensity of a helium–neon laser beam photometer, and expressed in terms of specific extinction area (SEA), with units of m<sup>2</sup>/kg. For RHR, the maximum value and the average to 180 s after ignition and the overall average values were determined. The total mass after the desired test time was calculated as a percentage of the initial sample mass.

## RESULTS AND DISCUSSION

### Characterization of the synthetic uncured organo-phosphorus epoxy

#### <sup>1</sup>H-NMR analysis

The chemical coupling of DOPO molecules into the epoxy backbone and the reaction of DGEBA or TGDDM and DOPO were confirmed primarily by <sup>1</sup>H-NMR spectroscopy analysis. Figure 1(a) and (b) show the <sup>1</sup>H-NMR of neat DOPO, DGEBA, and TGDDM. It also shows the reaction products of DOPO and DGEBA or TGDDM at 130°C and of DOPO and

DGEBA at 200°C. Very similar spectra were observed for the DGEBA–DOPO and TGDDM–DOPO reaction systems in terms of the DOPO peaks. DOPO reacts and covalently attaches to the epoxy backbone by reacting with the epoxide group by an etherification mechanism, creating a phosphorus-containing epoxy material, as explained and originally proposed by Lin.<sup>23</sup>

#### FTIR analysis

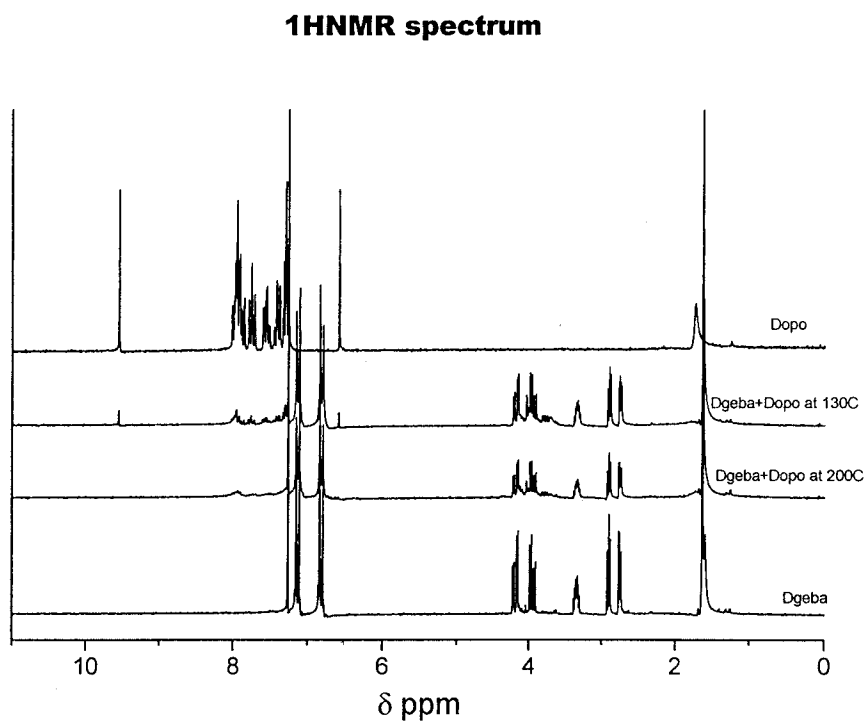
The mid FTIR spectra for the uncured DOPO–DGEBA and DOPO–TGDDM are shown in Figure 2(a) and (b), respectively. The strong absorption around 1240 cm<sup>-1</sup> corresponds to vibrations of the P=O moiety, which is characteristic of the DOPO molecule. The DOPO–DGEBA and DOPO–TGDDM reacted at 200°C showed very strong peaks at 1080–1130 and 750–860 cm<sup>-1</sup>, respectively, attributed to P–O–C stretching. Sharp peaks observed in the region of 1490–1520 cm<sup>-1</sup> are attributed to P–C (aromatic) stretching. A strong P–H absorption at 2400 cm<sup>-1</sup> was observed for DOPO, but completely disappeared when the DOPO was bonded with DGEBA. The absorption at about 3450 cm<sup>-1</sup> was attributed to the presence of hydroxyl molecule group. The strong absorption at 916 cm<sup>-1</sup> was attributed to the presence of oxirane ring.

Peaks in the reaction products of DOPO and epoxy, reacted at 130°C, were not as sharp as when combined at 200°C, suggesting that the DOPO–epoxy reaction was completed for 200°C reaction. From analysis of the FTIR spectra and <sup>1</sup>H-NMR spectra it is clear that the DOPO reacts readily with both DGEBA or TGDDM at 200°C and that the DOPO molecules remain at one end of the epoxy.

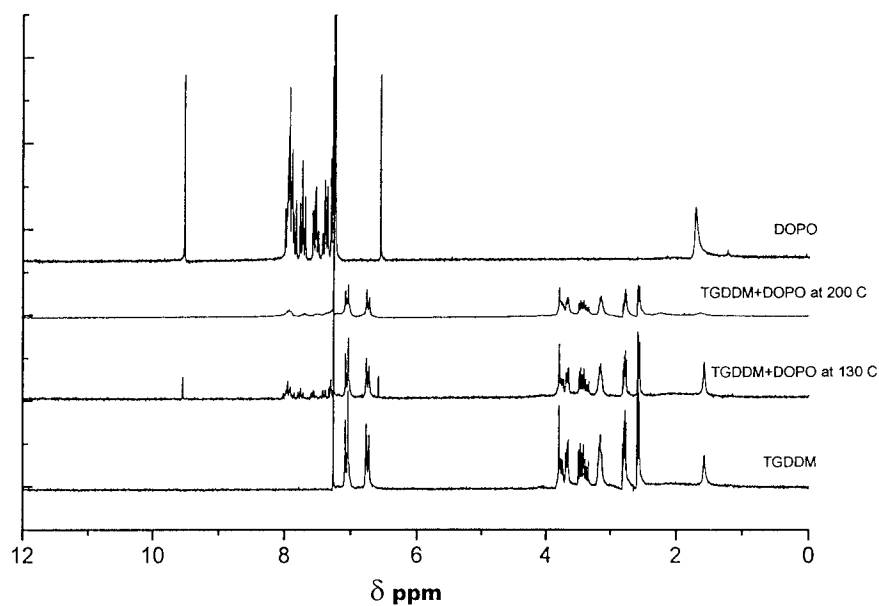
### Characterization of the cured organo-phosphorus epoxy compounds

#### Near IR

The near infrared spectra (n.i.r.) of initial reactants DGEBA and TGDDM, cured DGEBA and/or TGDDM, 3% phosphorus–DGEBA or TGDDM, and 3% phosphorus–7.5% clay–DGEBA or TGDDM are shown in Figure 3(a) and (b). Prominent epoxy peaks at 4523 cm<sup>-1</sup> and weak broad peaks at 5878–6068 cm<sup>-1</sup> are observed, as seen in the monomer in Figure 3(a). Similar peaks for TGDDM were observed at 4533 and 5885–5985 cm<sup>-1</sup>. The peak at 4523–4533 cm<sup>-1</sup> was attributed to a combination of the epoxide C–H fundamental at 3050 cm<sup>-1</sup> and CH<sub>2</sub> fundamental at 1460 cm<sup>-1</sup>. The peaks at 5885–5985 cm<sup>-1</sup> were attributed to the first overtones of the fundamental CH<sub>2</sub> and CH stretching, respectively. In the overtone region there were also aromatic C–H peaks at 4680 and 4617 cm<sup>-1</sup>, and aromatic N–H stretching at 5880 cm<sup>-1</sup> were observed.



(a)

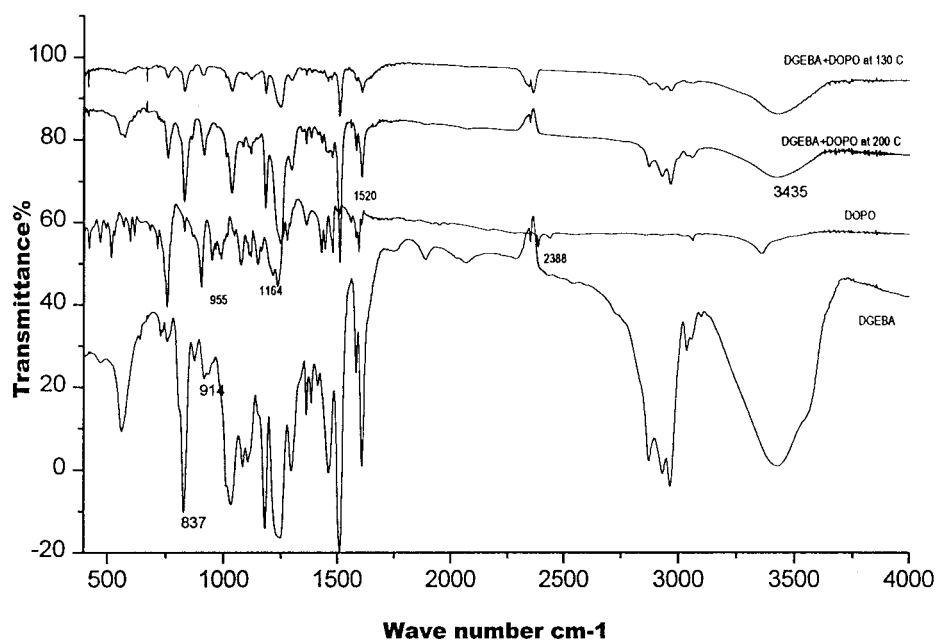


(b)

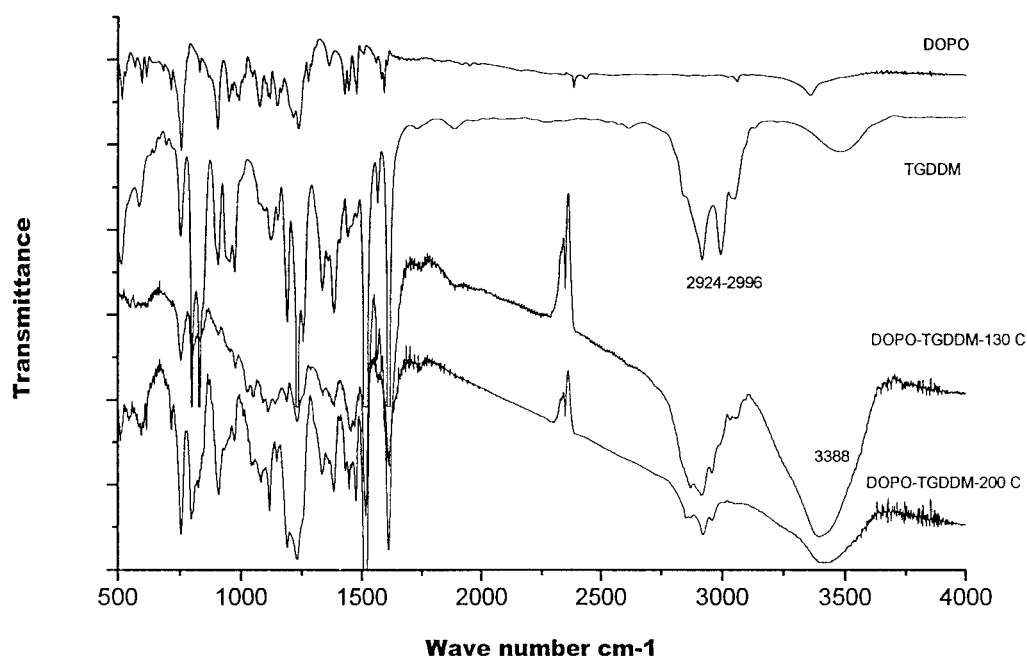
**Figure 1** <sup>1</sup>H-NMR spectra of (a) DGEBA, DOPO, and mixture of DGEBA and DOPO at different temperatures; and (b) TGDDM, DOPO, and mixture of TGDDM and DOPO at different temperatures.

The n.i.r. spectrum suggests that complete curing of DOPO–DGEBA or TGDDM occurs with amine, as evidenced by the disappearance of epoxide peak at

4523–4233  $\text{cm}^{-1}$ . Band peaks at 5984  $\text{cm}^{-1}$  of phosphorus–epoxy also confirm the presence of DOPO in the epoxy backbone. The peaks at 5230  $\text{cm}^{-1}$  in



(a)

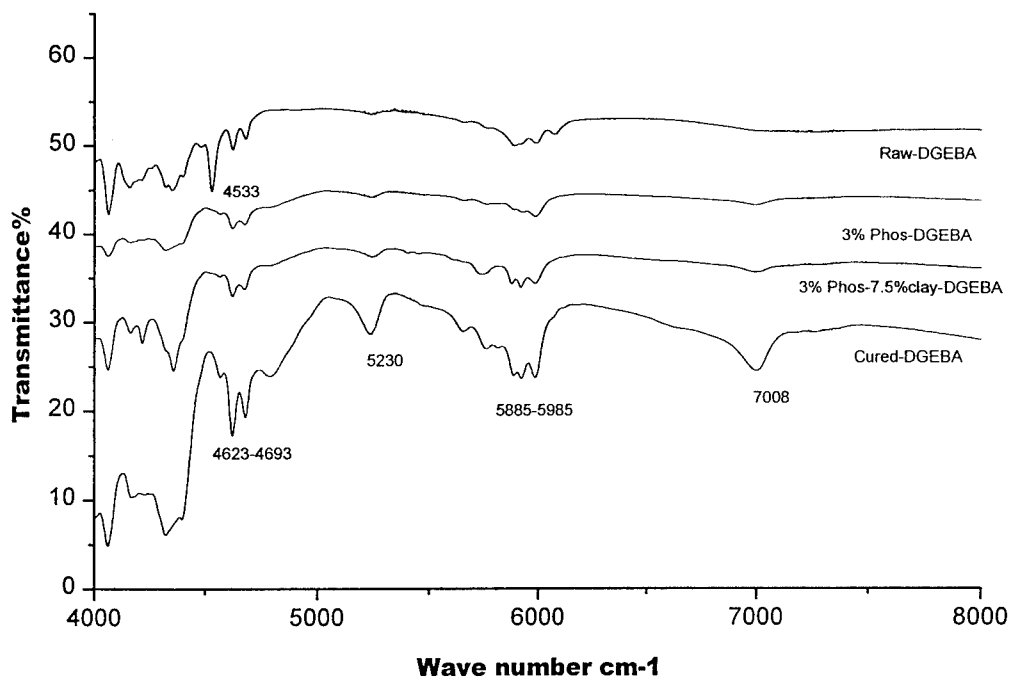


(b)

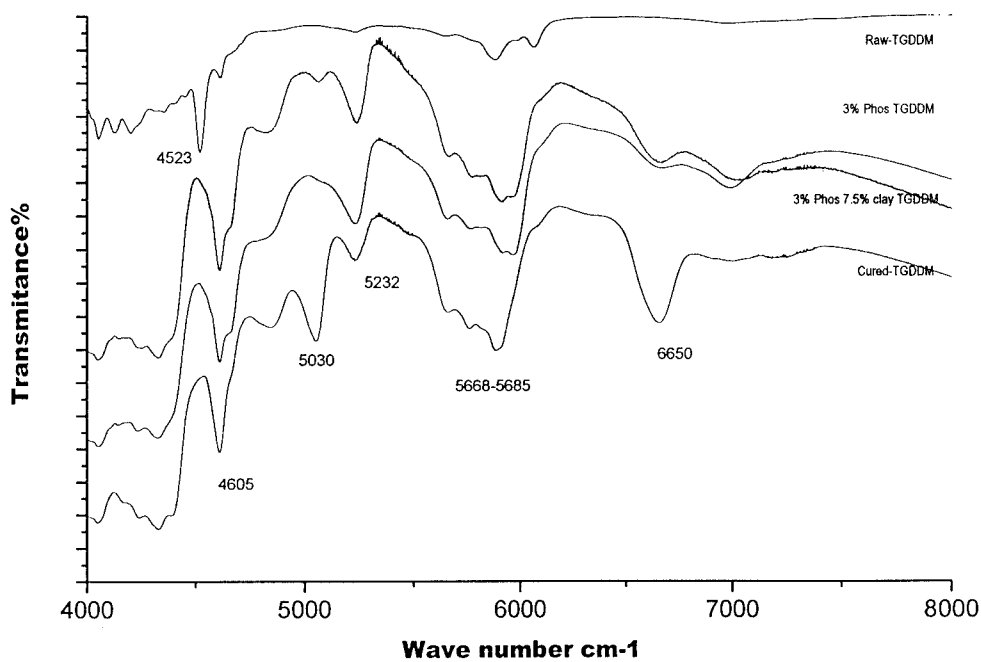
**Figure 2** FTIR spectra of (a) DGEBA, DOPO, and mixture of DGEBA and DOPO at different temperatures; and (b) TGDDM, DOPO, and mixture of TGDDM and DOPO at different temperatures.

DOPO-DGEBA and  $5030\text{ cm}^{-1}$  in DOPO-TGDDM cured samples are likely attributable to the presence of water and combinations of  $\text{CH}_2$  and  $\text{CH}$  bands.<sup>28</sup> This

peak decreased with increasing phosphorus content, completely disappearing in the 3% phosphorus-7.5% clay-TGDDM samples, for reasons not fully understood.



(a)



(b)

**Figure 3** Near infrared FTIR of (a) virgin DGEBA, cured DGEBA, 3% phosphorus-DGEBA, and 3% phosphorus-7.5% clay-DGEBA; and (b) virgin TGDDM, cured TGDDM, 3% phosphorus-TGDDM, and 3% phosphorus-7.5% clay-TGDDM.

### DSC analysis

To understand the effect of phosphorus and nano-clay additions to the curing behavior of the DGEBA or TGDDM epoxy systems, DSC measurements were made. Figure 4(a) and (b) show the DSC traces for the neat DGEBA/TGDDM-hardener reaction, 3% phosphorus-DGEBA/TGDDM, 7.5% clay-DGEBA/TGDDM, and for the reaction of blended 3% phosphorus-7.5% clay-DGEBA/TGDDM. It was found that both DGEBA and TGDDM show a decrease in the temperature location of the curing peaks, indicating an increase in reaction rate of the system. This can be explained by the fact that there is a strong catalytic effect of the organically modified clay on the cure reaction; such a catalytic effect of alkyl ammonium ions has been reported,<sup>29,30</sup> where the ammonium ion has a Bronstedt-acid catalyzing effect on the curing reaction. It is clear from Figure 4(a) and (b) that DGEBA is affected to a greater degree by the catalyzing effect of the organo-clay than by the tetrafunctional TGDDM. Recent results<sup>30</sup> have shown for DGEBA resin, modified with organo-clay, that the resin-hardener intercalates into the clay galleries and causes swelling during the mixing, with greater separation of layers and a degree of exfoliation occurring during cure.<sup>31</sup> The situation is not so clear for the phosphorus-modified systems. A decrease in curing temperature was observed in 3% phosphorus-DGEBA (increased reactivity), whereas an increase in curing temperature was observed in the 3% phosphorus-TGDDM system (reduced reactivity). In general, an electron-donating group in an amine curing agent increases the electron density of the amine group and thus increases the reactivity of the amine group with an epoxide ring.<sup>10</sup> However, if a P=O group is also present, its electron-withdrawing nature reduces the electron density of the amine group, thus decreasing the strength of the nucleophilic attack on the oxirane ring of the epoxy resins and therefore the epoxy-amine reaction.<sup>32</sup> The high reactivity of a phosphorus-containing epoxy with amine possibly results from a similar electronic effect, but in reverse. In this reaction P=O group acts as an electron-withdrawing group within the epoxy, reducing the electron density of oxirane rings and thus facilitates nucleophilic attack by the amine species, thereby accelerating the reaction kinetics. In 3% phosphorus in TGDDM system an increase in the maximum of the curing exotherm might also be attributed to decreased monomer mobility. The incorporation of bulky DOPO with two aromatic units and TGDDM (with such benzene rings) has very high activation energy and thus the curing rate is decreased. The increase in curing rate upon addition of organo-modified clay to the 3% phosphorus-TGDDM system is attributed, once again, to the catalytic effects of the organic species in the clay.

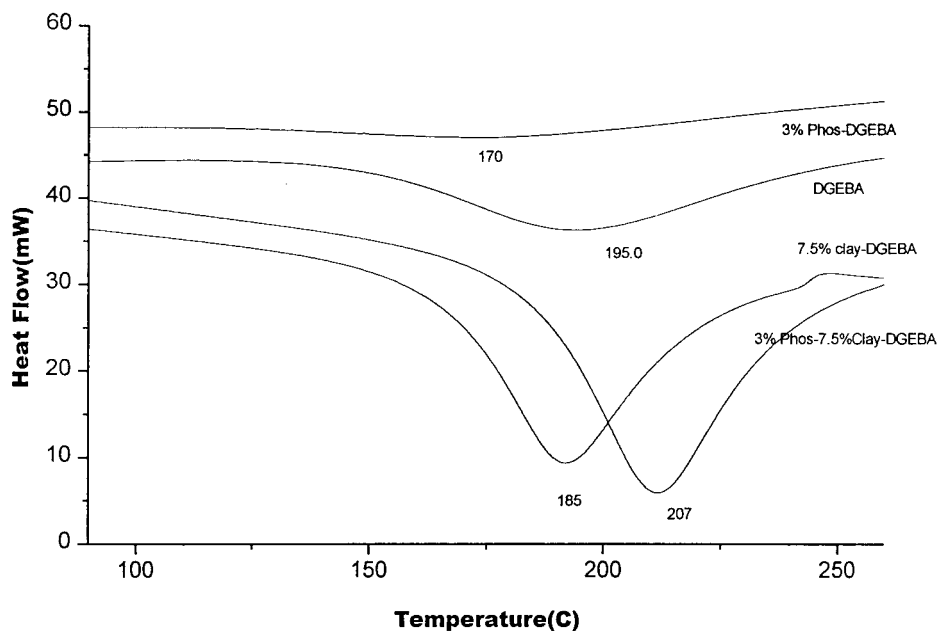
### Morphology

An important aspect of the work is the inclusion of clay into the systems, whether they are simple epoxies (DGEBA or TGDDM) and amines or similar systems with phosphate moieties incorporated. The key objective with such clay in nanocomposites is to determine the change in degree of clay layer spacing that occurs and its effect on degradation of materials and fire-retardant properties. This can be readily done to some degree by XRD in which the 001 peak position of the clay is indicative of the *d*-spacing between the layers. The degree to which XRD can measure increased intercalation and/or eventual exfoliation (if the layers are fully delaminated) depends on the lower angles obtainable by available equipment but usually is in the order of 70–80 Å. The remaining of any clay tactoids that still exist with some degree of lateral registration is often better assessed by other techniques such as TEM.

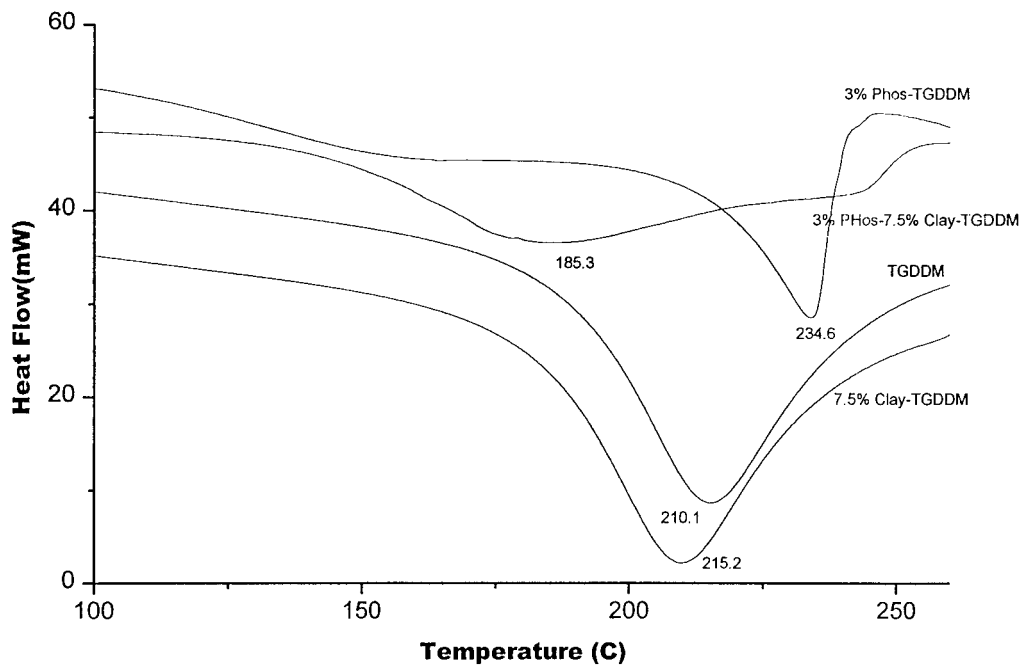
Figure 5(a) shows the typical XRD pattern of 7.5% clay and DGEBA and 3% phosphorus-7.5% clay-DGEBA obtained for nanocomposites materials. There are characteristic peaks of clay in both nanocomposites, showing *d*(001) spacing of 39.27 Å, larger than that of the usual clay at *d*(001) of 23 Å. The data clearly suggest that the clay particles are intercalated in DGEBA and phosphorus-DGEBA equally well. The intercalated structure of clay-DGEBA was further examined by TEM micrographs, discussed later.

In contrast to the DGEBA system, the 7.5% clay-TGDDM system in Figure 5(b) did not show a distinct clay peak in the *d*(001) spacing region. However, the presence of clay in the phosphorus-TGDDM system showed clay peaks *d*(001) and *d*(002) spacing at 38.41 and 18.4 Å, respectively. This indicates that the presence of the phosphorus moiety in epoxy decreases the exfoliation of clay particles, possibly attributed to the enhanced curing of epoxy at the side of the galleries because of the presence of phosphorus, as observed by the increase in reaction rate (decrease in location of exothermic peak) in Figure 4(b). Becker et al.<sup>33</sup> also pointed out that the intercalation or exfoliation of clay occurs in epoxy composites during the early stage of cure. Lan et al.<sup>34</sup> suggested that a possible mechanism of polymer swelling in the clay galleries is by self-polymerization of the epoxy resin catalyzed by the acidity of the alkyl ammonium ion within the clay galleries. With further polymerization (during cure), the epoxy molecules are enabled to enter between the clay layers and cause the clay layers to push apart from each other. Berglund et al.<sup>35</sup> also suggested that high surface energy of the clay attracts the polar species of the epoxy molecules so that they diffuse readily into the layers. The presence of a large phosphorus moiety may aid in pushing the clay layers apart from



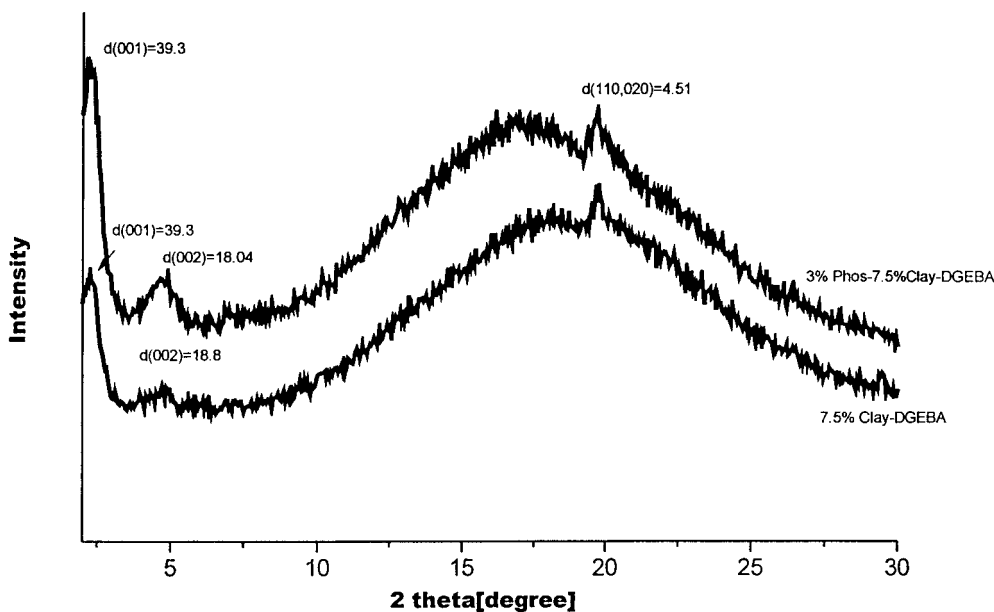


(a)

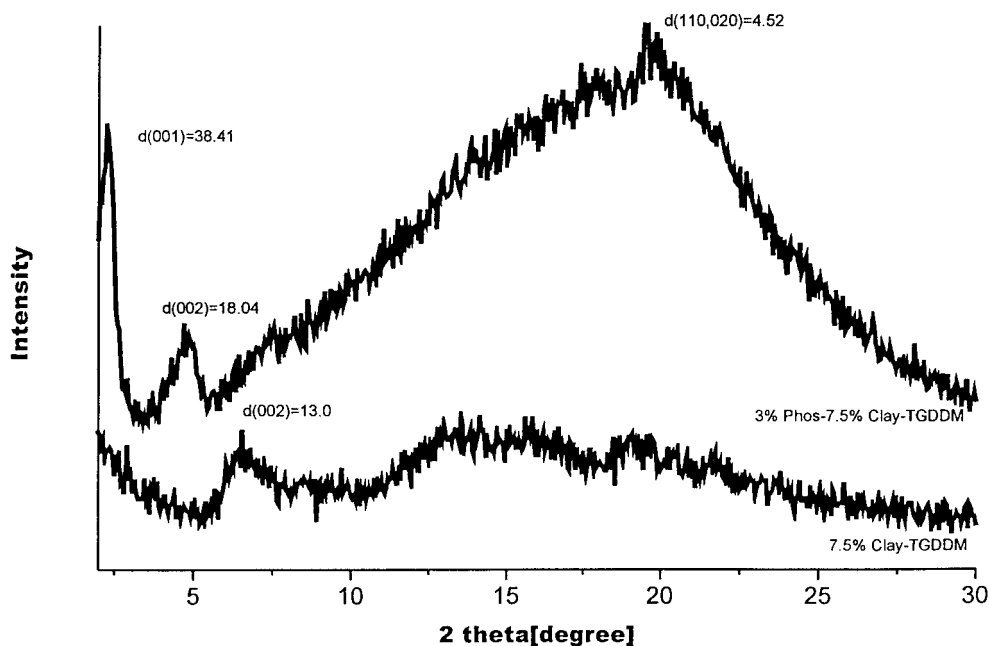


(b)

Figure 4 DSC spectra of (a) DGEBA, 3% phosphorus-DGEBA, 7.5% clay-DGEBA, and 3% phosphorus-7.5% clay-DGEBA; and (b) TGDDM, 3% phosphorus-TGDDM, 7.5% clay-TGDDM, and 3% phosphorus-7.5% clay-TGDDM.



(a)



(b)

**Figure 5** XRD spectra of (a) 7.5% clay-DGEBA and 3% phosphorus-7.5% clay-DGEBA; and (b) 7.5% clay-TGDDM and 3% phosphorus-7.5% clay-TGDDM.

each other. The intercalated/exfoliated structures of clay-TGDDM or clay-phosphorus-TGDDM system were further examined by TEM micrographs.

TEM was taken for two sets of nanocomposites with clay and clay-phosphorus DGEBA and TGDDM systems. Figure 6(a) and (b) show the DGEBA-clay nano-

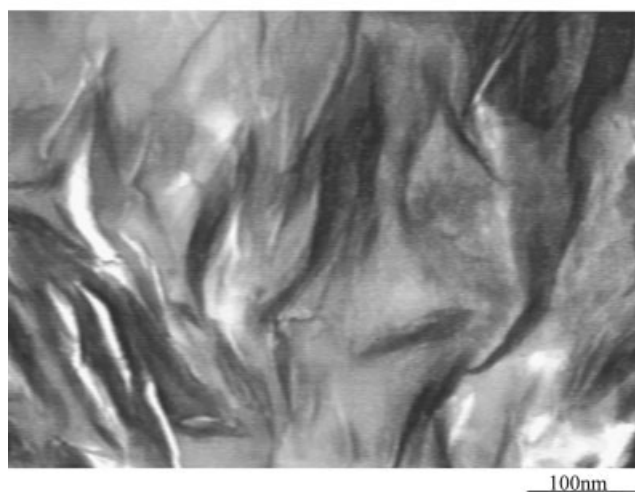
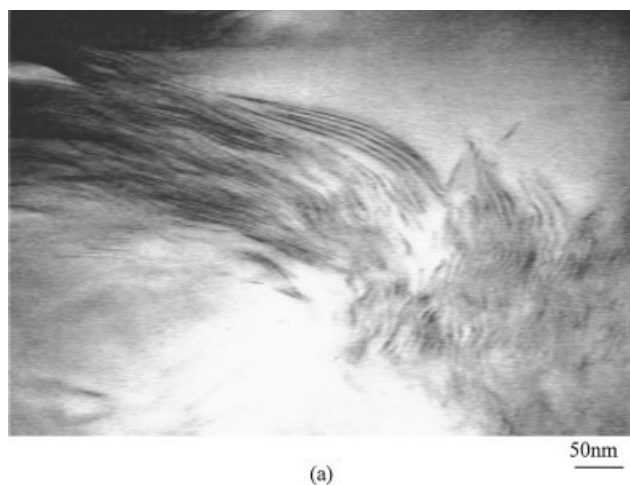


**Figure 6** TEM micrographs of (a) 7.5% clay-DGEBA and (b) 3% phosphorus-7.5% clay-DGEBA nanocomposites.

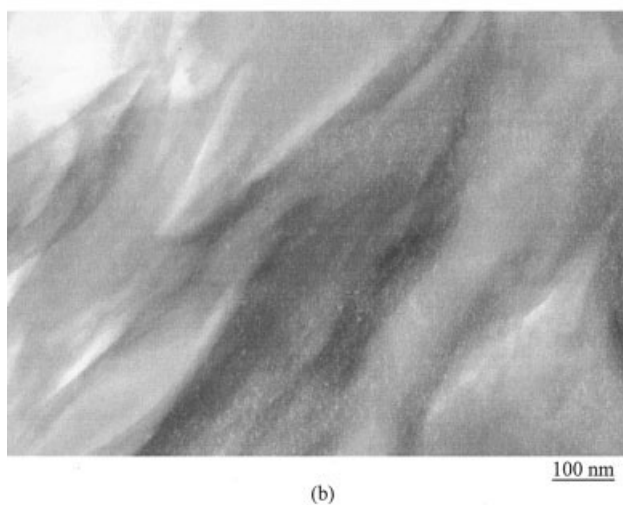
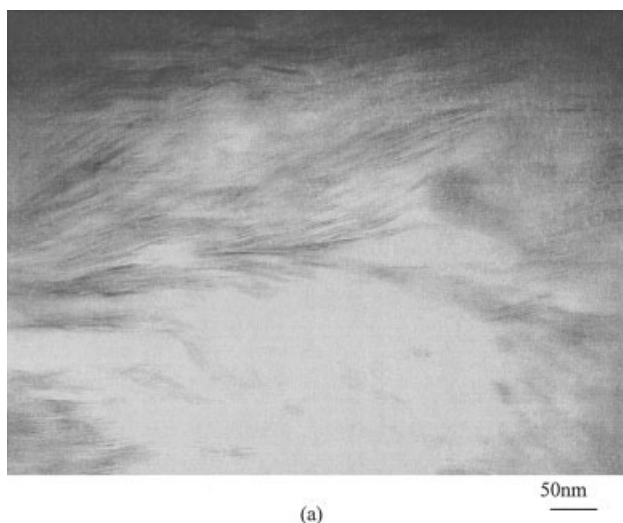
composites and DGEBA-clay-phosphorus nanocomposites. The clay platelets in the DGEBA-clay micrograph show better parallel orientation with increasing  $d$ -spacing than that of DGEBA-clay-phosphorus nanocomposites. This suggests that the clay platelets are highly intercalated. However, small number of single platelets can also be observed that were delaminated from the main clay structure.

Figure 7(a) and (b) show the clay dispersion in TGDDM and phosphorus-TGDDM system, respectively. The exfoliated, rather than intercalated, nature of clay was observed in the clay-TGDDM system. However, an intercalated clay structure with increasing  $d$ -spacing was observed in the phosphorus-clay-TGDDM system as the parallel orientation of clay was observed in Figure 7(b). This might be attributable to the increase of viscosity of epoxy resin by adding phosphorus compound into the epoxy system, which prevents easy swelling of epoxy resins into the clay galleries.

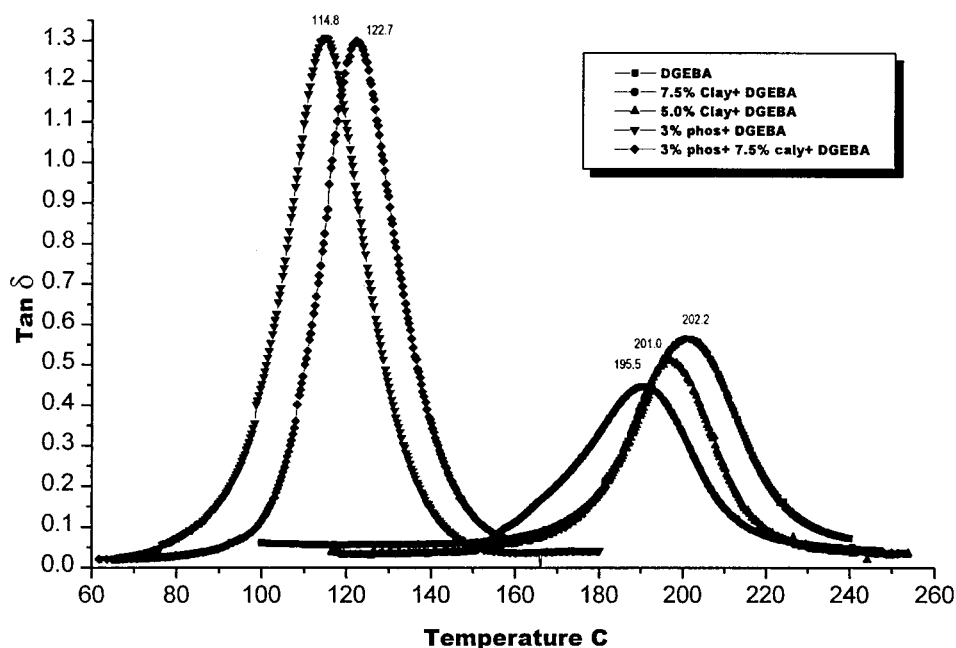
### Thermal properties of composites

#### Dynamic mechanical thermal analysis (DMTA)

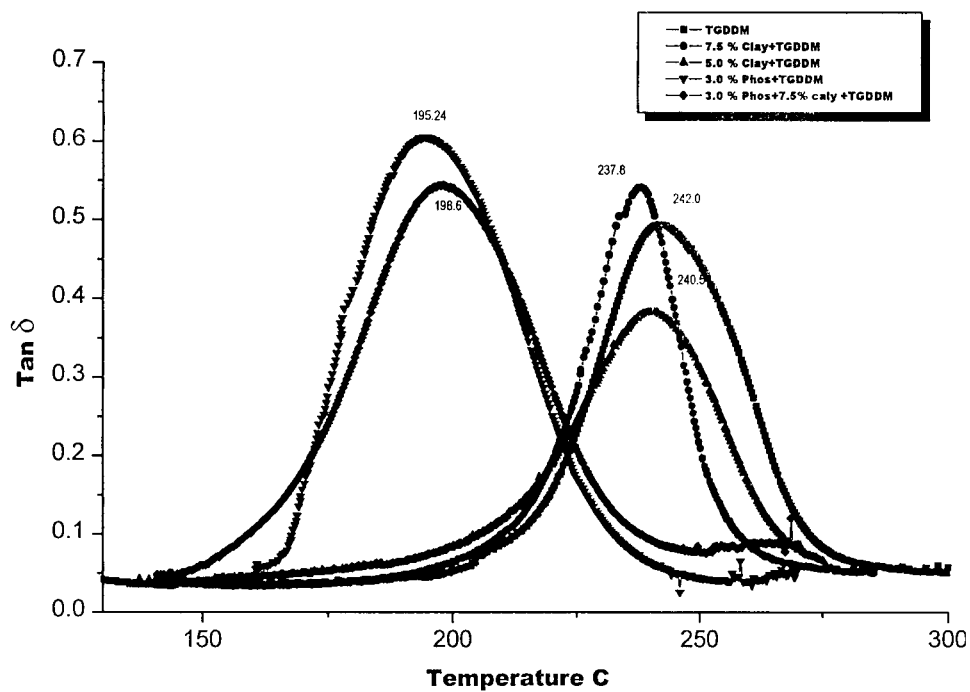
The glass-transition temperature ( $T_g$ ) and dynamic-mechanical properties of DGEBA, TGDDM, and modified DGEBA and TGDDM were determined. Figure 8(a) and (b) show the  $\tan \delta$  spectra from dynamic mechanical analyses of the cured DGEBA and TGDDM systems, respectively. Both the DGEBA and TGDDM systems showed a decrease in  $T_g$  with the addition of clay. The effect on the  $T_g$  of clay addition has been widely studied,<sup>38-40</sup> with many investigators reporting an increase in  $T_g$  values,<sup>31,40</sup> whereas others found a slight decrease or no change.<sup>41,42</sup> Kormann et al.<sup>43</sup> and Becker et al.<sup>44</sup> reported a decrease in  $T_g$  for higher functionality epoxy resins similar to the results reported here. It is suggested that the decrease in  $T_g$  of clay-modified nanocomposites is attributed to the interference of the clay with crosslink density, issues such as epoxy homopolymerization and the plastici-



**Figure 7** TEM micrographs of (a) 7.5% clay-TGDDM and (b) 3% phosphorus-7.5% clay-TGDDM nanocomposites.

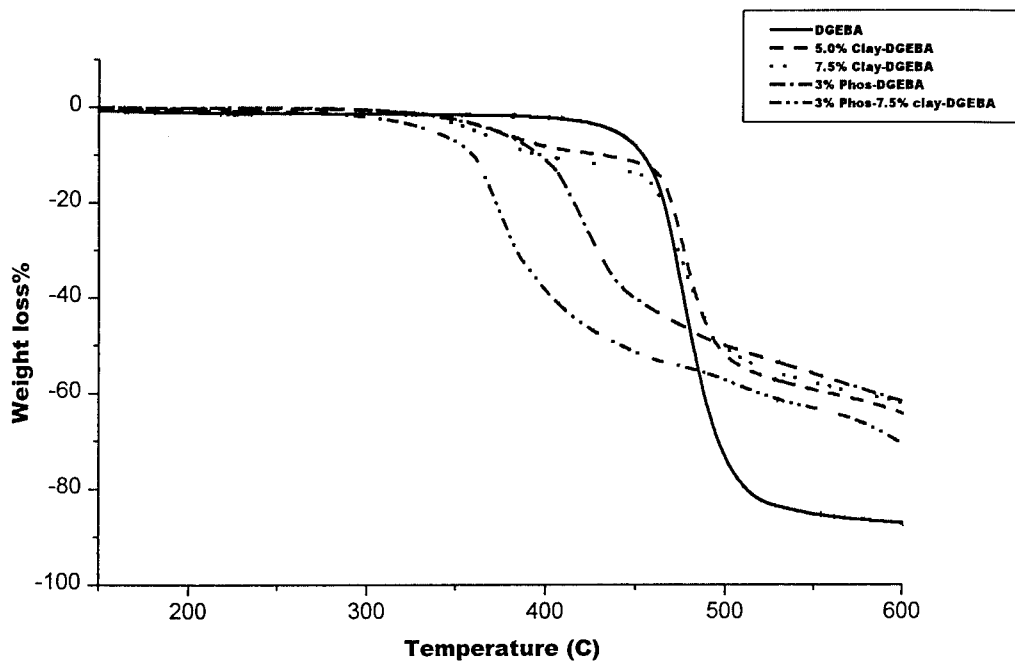


(a)

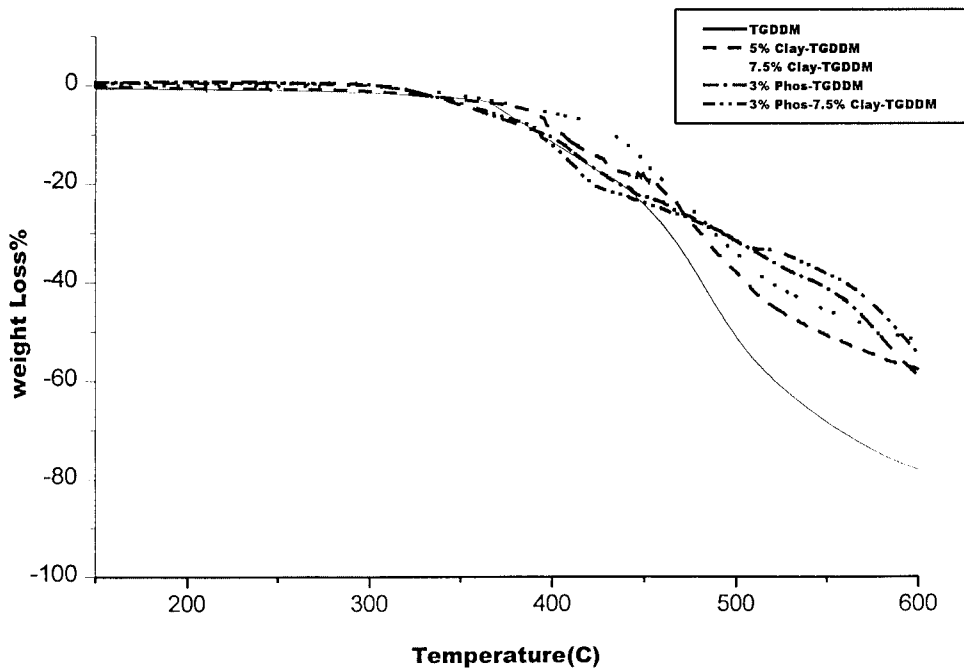


(b)

**Figure 8** DMTA spectra of (a) cured DGEBA, 3% phosphorus-DGEBA, 5% clay-DGEBA, 7.5% clay-DGEBA, and 3% phosphorus-7.5% clay-DGEBA; and (b) cured TGDDM, 3% phosphorus-TGDDM, 5% clay-TGDDM, 7.5% clay-TGDDM, and 3% phosphorus-7.5% clay-TGDDM.



(a)



(b)

**Figure 9** TGA spectra of (a) cured DGEBA, 3% phosphorus-DGEBA, 5% clay-DGEBA, 7.5% clay-DGEBA, and 3% phosphorus-7.5% clay-DGEBA; and (b) cured TGDDM, 3% phosphorus-TGDDM, 5% clay-TGDDM, 7.5% clay-TGDDM, and 3% phosphorus-7.5% clay-TGDDM.

TABLE II  
Thermal Properties of Epoxy Resin and Modified Epoxy Resin Composite

Material	Temperature of weight loss at 10%	Char yield (%)		LOI
		400°C	600°C	
Pure DGEBA	450	100	14.0	25.0
3% Phos-DGEBA	400	90	42.0	33.0
5.0% Clay-DGEBA	420	92	38.0	32.7
7.5% Clay-DGEBA	405	90	40.0	34.5
7.5% Clay-3%Phos-DGEBA	360	60	28.0	28.7
Pure TGDDM	400	90	22.0	26.3
3% Phos-TGDDM	395	91	42.0	34.3
5.0% Clay-TGDDM	420	93	44.0	35.1
7.5% Clay-TGDDM	445	97	48.0	36.7
7.5% Clay-3% Phos-TGDDM	405	90	44.0	35.1

zation resulting from the presence of alkylammonium ion in clay. We also observed the phosphorus addition in this work, that both DGEBA or TGDDM exhibited much lower glass-transition temperatures. Chiu et al.<sup>45</sup> also observed the lowering of  $T_g$  of the composites on addition of phosphorus-containing compounds in epoxy resins. Wang et al. reported similar results and proposed that higher epoxy equivalent weight (EEW) of organo-phosphorus epoxy reduces the crosslink density (some reactive epoxy groups are substituted), subsequently decreasing the glass-transition temperature.<sup>23</sup> The lower crosslink density is confirmed by the greater height of the delta relaxational observed in Figure 8(a) and (b), which is indicative of greater relaxation strength. It may have been expected that the decrease in  $T_g$  ( $\sim 50$ – $80^\circ\text{C}$ ) may not have been as great because of the restrictive nature of the bulky DOPO compound that would be expected to hinder molecular rotation and thus increase  $T_g$ . Clearly in this

case, therefore, it can be asserted that the reduction in crosslink density outweighs that expected increase as a result of the bulky DOPO groups to decrease  $T_g$ . Addition of 7.5 wt % clay to the phosphorus-modified DGEBA or TGDDM system was found to lead to a modest increase in  $T_g$ . The addition of clay to either DGEBA or TGDDM also caused a decrease, the reason for which is not clear, and may be attributable to some degree of association between the clay and phosphorus moieties. Nonetheless, the change is not significant.

#### Thermogravimetric analysis (TGA)

The fire performance of a material is associated with processes occurring in both the condensed and gaseous phases, both relating to the thermal degradation of material. To examine the effect of addition of phosphorus, clay, and the two in combination on the thermal stability of cured DGEBA and TGDDM resins, thermogravimetric experiments were performed. Figure 9(a) and (b) show the weight loss for the unmodified epoxies and phosphorus-, clay-, and phosphorus-clay-modified epoxy systems. In unmodified cured DGEBA system in Figure 9(a) degradation starts at around  $420^\circ\text{C}$  with the rate of degradation significantly increasing above  $450^\circ\text{C}$  and a char yield of 14% remaining at  $600^\circ\text{C}$ . On addition of 5 and 7.5% clay in DGEBA, the initial degradation temperature occurs slightly lower at  $340^\circ\text{C}$  and the rate of degradation maxima increases to about  $465^\circ\text{C}$ , with a greater char yield of 38–40% at  $600^\circ\text{C}$ . The results clearly indicate that the onset of degradation occurs at slightly lower temperature, attributed to the Hoffman-elimination of the alkyl ammonium chain and char formation, is enhanced by some 20%, even though only 5.0 or 7.5 wt % clay is added. Clearly the clay forms a barrier to degradation and stabilizes the char layer. In contrast, DGEBA modified with 3 wt % phosphorus, or phosphorus-clay show an earlier onset degradation temperature after  $300^\circ\text{C}$  and char yields of 42 and 28% for

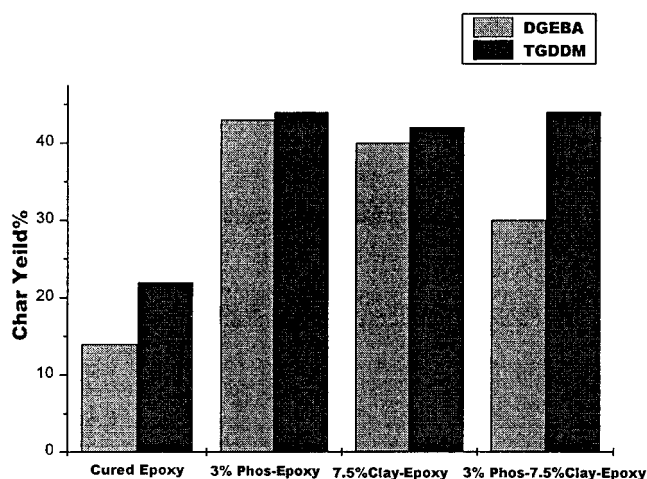
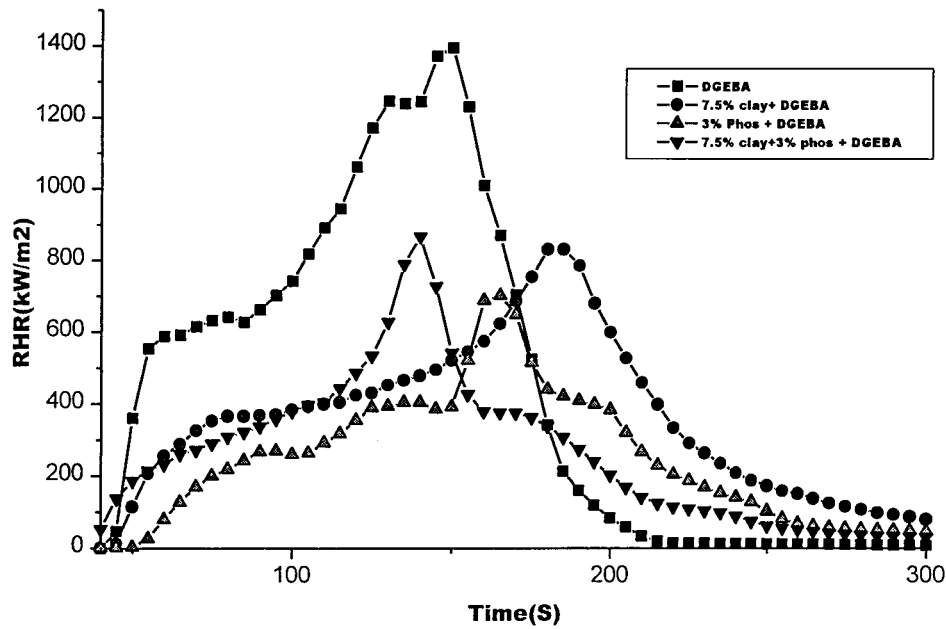
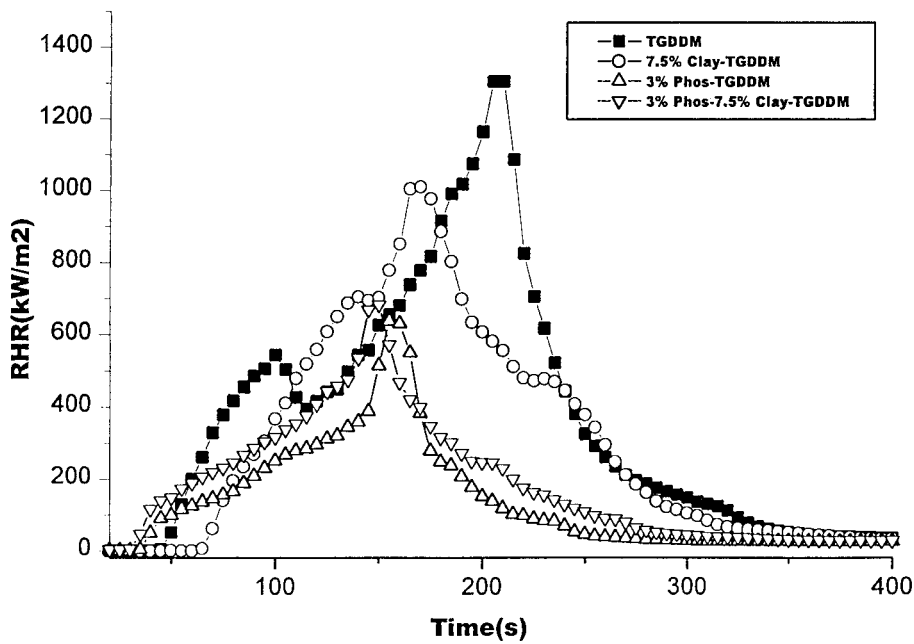


Figure 10 Histogram of char yield of cured DGEBA, 3% phosphorus-DGEBA, 7.5% clay-DGEBA, and 3% phosphorus-7.5% clay-DGEBA; and cured TGDDM, 3% phosphorus-TGDDM, 7.5% clay-TGDDM, and 3% phosphorus-7.5% clay-TGDDM.



(a)



(b)

**Figure 11** RHR spectra of (a) DGEBA, 3% phosphorus–DGEBA, 7.5% clay–DGEBA, and 3% phosphorus–7.5% clay–DGEBA; and (b) cured TGDDM, 3% phosphorus–TGDDM, 7.5% clay–TGDDM, and 3% phosphorus–7.5% clay–TGDDM.

3% phosphorus–DGEBA and 3% phosphorus–7.5% clay–DGEBA, respectively. The reason that the onset degradation temperatures of the phosphorus–DGEBA or phosphorus–clay–DGEBA resins are lower than

those of neat epoxy is likely to be attributed to the decomposition of P–O–C bonds.<sup>36,37</sup> While burning, the phosphorus-containing groups degrade at an early onset temperature and form a phosphorus-rich resi-

TABLE III  
Cone Calorimetric Data Measured with an Irradiance of 50 k Wm<sup>-2</sup>

Fire property	DGEBA	7.5% Clay-DGEBA	3% Phos-DGEBA	7.5% Clay-DGEBA	3% Phos-DGEBA	TGDDM	7.5% Clay-TGDDM	Phos-TGDDM	3% TGDDM	7.5% Clay-TGDDM	3% Phos-TGDDM
Time to ignition (s)	65	47	55	41	41	50	49	39	39	49	36
Peak HRR (kW/m <sup>2</sup> )	1396	857	702	867	867	1304	1090	637	637	1090	682
Average HRR (kW/m <sup>2</sup> )	399.8	372.5	291.1	321.3	321.3	485.3	501.9	229	229	501.9	275
Average HRR at 180 s	501	472.0	336.3	290	290	645.5	623.7	229.7	229.7	623.7	275.5
Time to maximum HRR (s)	155	145	165	140	140	210	170	155	155	170	150
Average effective heat of combustion (MJ/kg)	21.2	22.4	15.80	14.2	14.2	23.72	25.7	14.2	14.2	25.7	14.9
Average smoke obscuration (m <sup>2</sup> /kg)	1234.0	1228.5	1865.3	1856	1856	1129.4	1174.7	1458.5	1458.5	1174.7	1728.7
Average CO yield (kg/kg)	0.0454	0.0464	0.097	0.08	0.08	0.052	0.053	0.0963	0.0963	0.053	0.0903
Average CO <sub>2</sub> yield (kg/kg)	1.48	1.55	1.077	0.83	0.83	1.746	1.877	0.79	0.79	1.877	0.82
Total heat evolved (MJ/m <sup>2</sup> )	89.65	98.72	64.05	75.0	75.0	138.3	122.9	48.23	48.23	122.9	66.11
Mass loss (%)	82.8	86.5	64.6	82.3	82.3	78.9	78.6	57.6	57.6	78.6	74.5

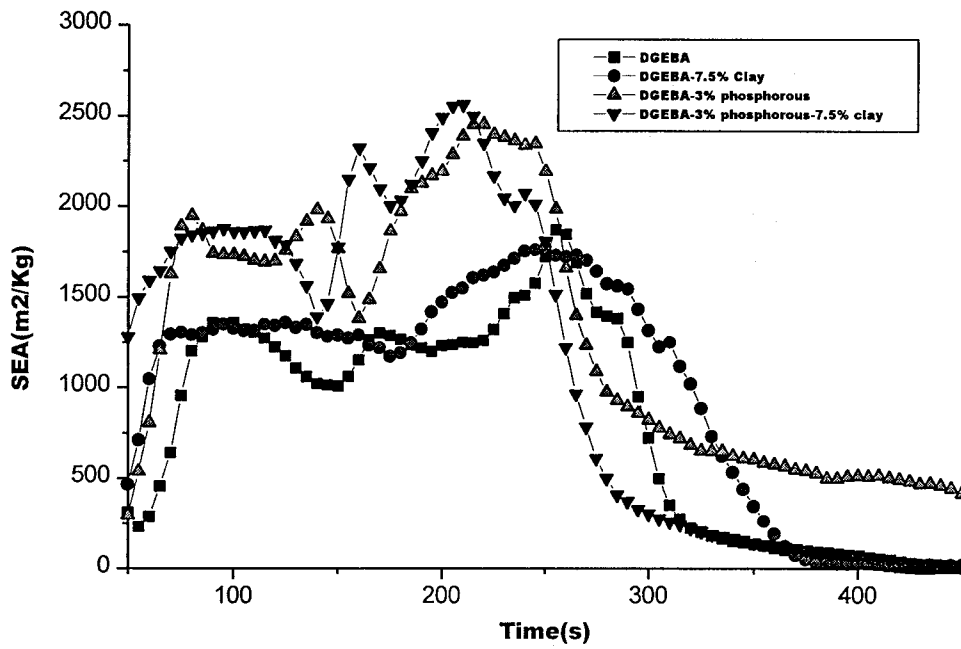
due and prevent a significant decrease in further degradation. A higher char yield is thus probably responsible and may be explained by a condensed phase mechanism used as an indicator for fire retardance of materials.

Similar degradative behavior was observed for the TGGDM epoxy system. Phosphorus-containing TGDDM was found to begin degradation earlier than that of pure TGDDM or clay-TGDDM system. The char yield of TGDDM alone at 600°C was found to be 22%. Addition of phosphorus or clay was significantly improved up to 48% char yield. As for DGEBA, the effect of thermal properties can be explained because of the presence of clay nanolayers in the epoxy, which acts as a physical barrier preventing the evolution of volatile degradation products from the matrix. A higher char yield can therefore be expected to increase the flame retardance. In our previous article<sup>17</sup> it was shown that the limiting oxygen index (LOI) could be calculated from the obtained TGA graphs. In this article, LOI values of DGEBA, phosphorus-modified DGEBA, clay-modified DGEBA, and phosphorus-clay-modified DGEBA were found to be 25.5, 33.0, 34.5, and 28.7, respectively, indicating that modified epoxy composites are potentially better flame retardant materials than the pure DGEBA. However, a synergistic effect of phosphorus and clay addition on LOI was not observed. Similarly, in the TGDDM system LOI values were found to be 26.3, 34.3, 35.1, 36.7, and 35.1 for unmodified TGDDM, phosphorus-modified TGDDM, clay-modified TGDDM, and phosphorus-clay-modified TGDDM, respectively. For the DGEBA system, the synergistic effect of phosphorus and clay addition on LOI in the TGDDM system was not observed. Table II shows the thermal properties of pure DGEBA, TGDDM, and modified DGEBA and TGDDM. Figure 10 shows the char yield percentage of DGEBA or TGDDM epoxy and modified epoxy composites. Increases in char formation were observed in both DGEBA and TGDDM systems when clay and phosphorus were added. Maximum char yields were observed in 3% phosphorus-epoxy composites in both DGEBA and TGDDM. Synergistic effects of clay and phosphorus addition on char formation were not observed.

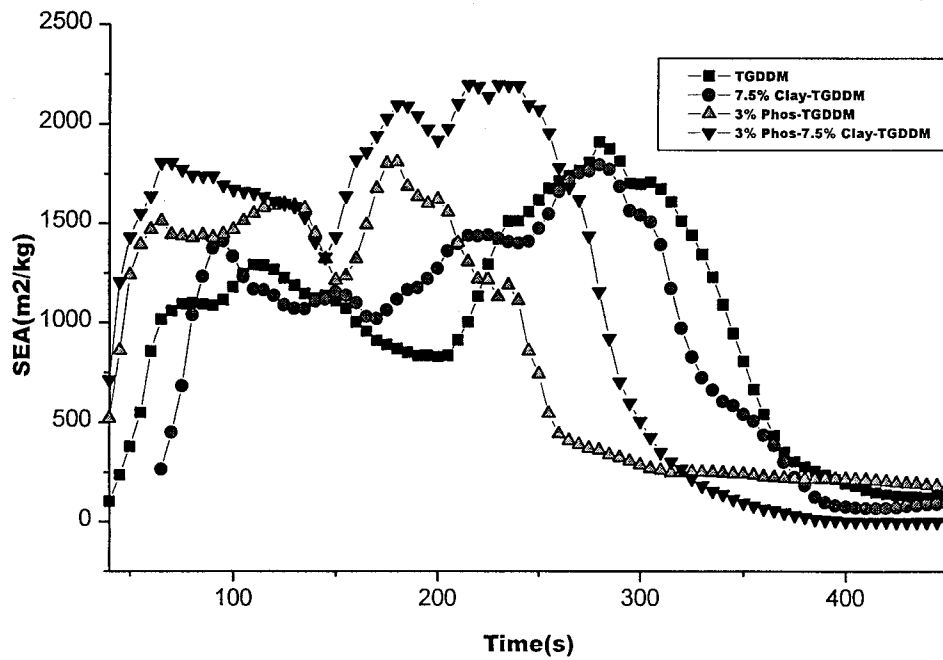
Flammability testing by cone calorimetry

The cone calorimeter provides important information on the combustion behavior of a material under ventilated conditions. The peak rate of heat release of a material is one of the important factors to determine the potential behavior during fire. Figure 11(a) and (b) show the rate of heat release (RHR) of DGEBA or TGDDM and modified DGEBA and TGDDM variation with time at a heat flux of 50 kW/m<sup>2</sup>. The peak rate of heat release for DGEBA is high at around 1400 kW/





(a)

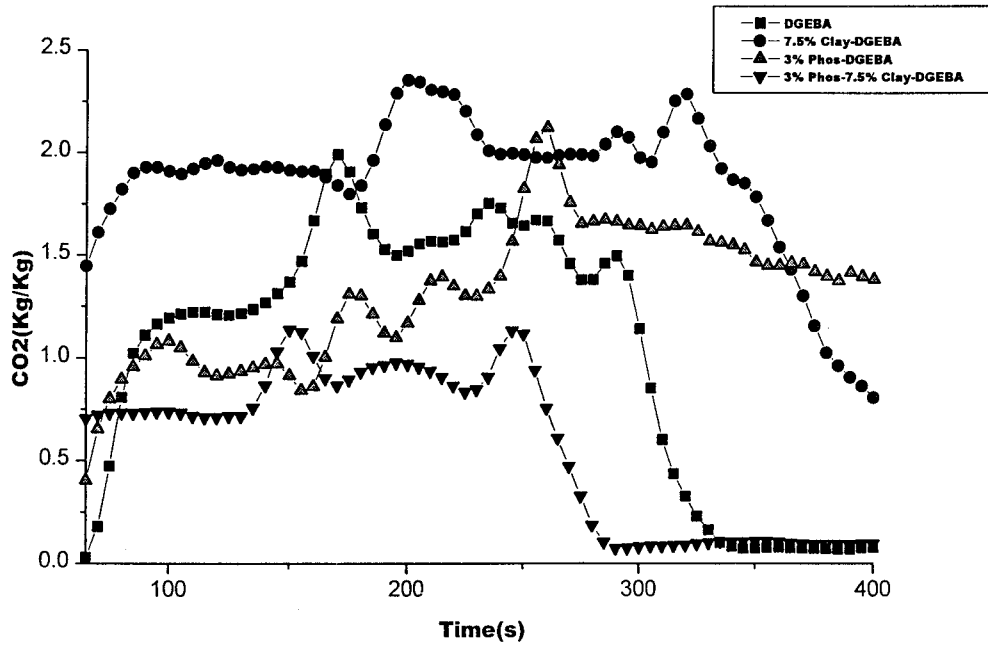


(b)

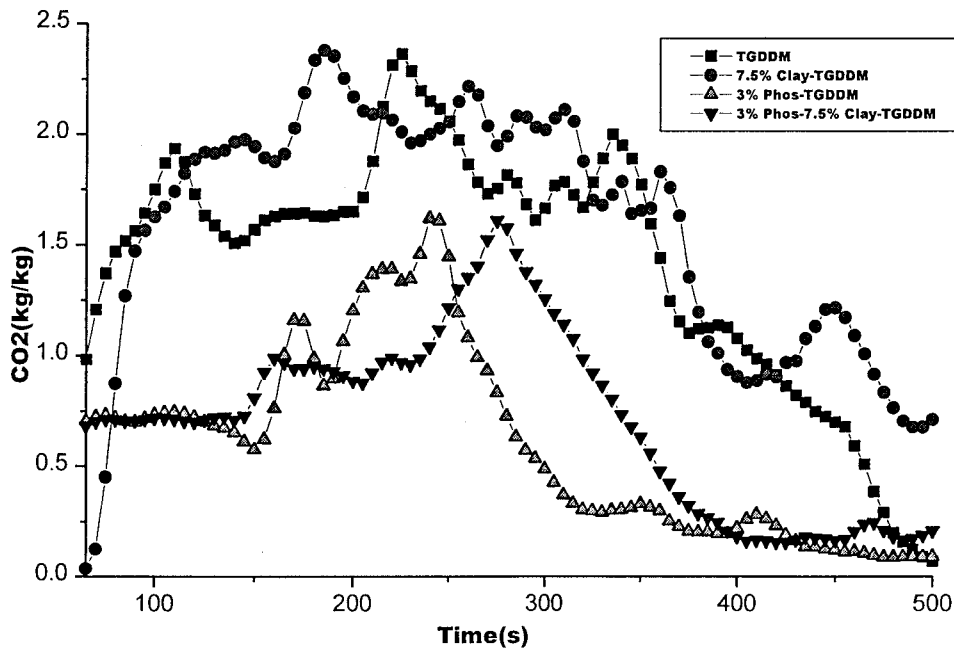
**Figure 12** SEA spectra of (a) DGEBA, 3% phosphorus-DGEBA, 7.5% clay-DGEBA, and 3% phosphorus-7.5% clay-DGEBA; and (b) cured TGDDM, 3% phosphorus-TGDDM, 7.5% clay-TGDDM, and 3% phosphorus-7.5% clay-TGDDM.

m<sup>2</sup>. However, 7.5% clay-modified DGEBA has a lower peak rate of release at 857 kW/m<sup>2</sup>, which is significantly reduced to 40% compared to that of unmodified

DGEBA. In contrast, DGEBA modified with phosphorus showed a peak release rate at 702 kW/m<sup>2</sup>, which is 50% lower than that of unmodified DGEBA. The



(a)

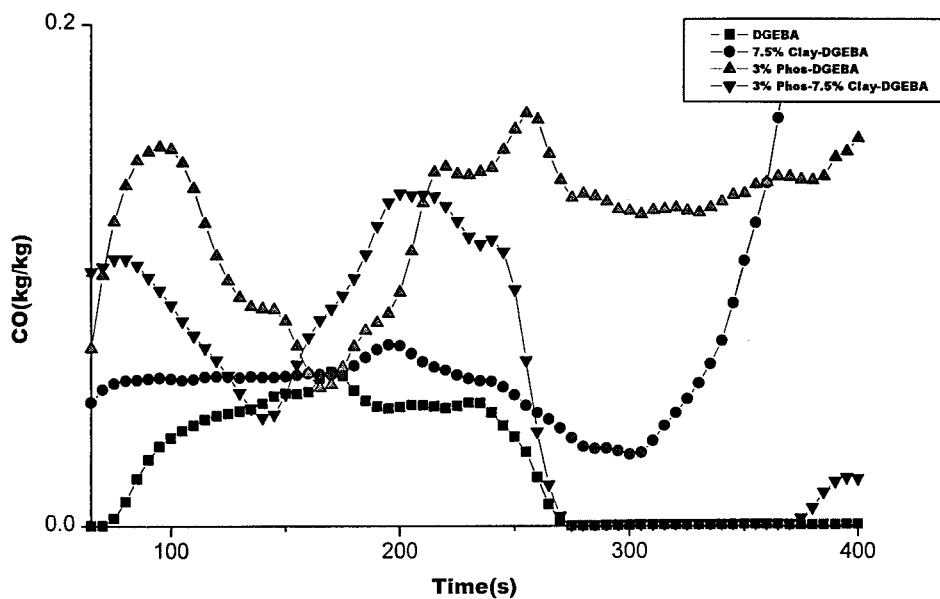


(b)

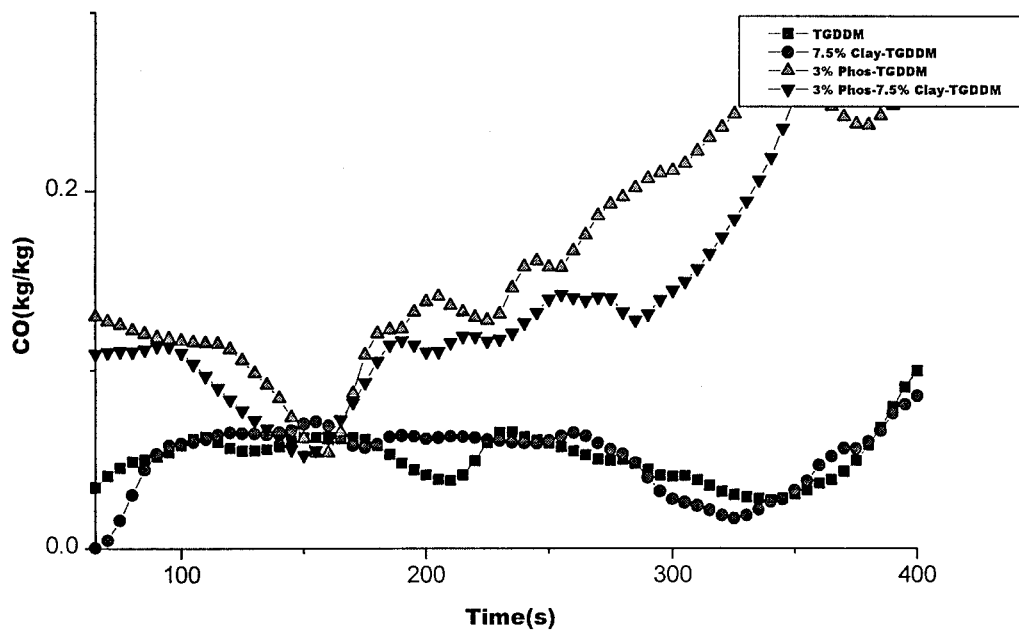
**Figure 13** CO<sub>2</sub> emission spectra of (a) DGEBA, 3% phosphorus-DGEBA, 7.5% clay-DGEBA, and 3% phosphorus-7.5% clay-DGEBA; and (b) cured TGDDM, 3% phosphorus-TGDDM, 7.5% clay-TGDDM, and 3% phosphorus-7.5% clay-TGDDM.

significant RHR reduction is attributed to incorporation of the phosphorus moiety. An increase in flame retardance in phosphorus-modified DGEBA also

comes from the residual masses or char obtained during firing. On the other hand, DGEBA modified with both phosphorus and clay has a peak heat release rate



(a)



(b)

**Figure 14** CO emission spectra of (a) DGEBA, 3% phosphorus-DGEBA, 7.5% clay-DGEBA, and 3% phosphorus-7.5% clay-DGEBA; and (b) cured TGDDM, 3% phosphorus-TGDDM, 7.5% clay-TGDDM, and 3% phosphorus-7.5% clay-TGDDM.

at 866 kW/m<sup>2</sup>, 38% lower than that of unmodified DGEBA. Thus the synergistic effect of phosphorus and clay in terms of heat release was not observed. However, no synergistic effect (or worse result) was ob-

served in terms of time when clay and phosphorus were both added. A higher percentage of mass residue or char indicates a condensed-phase flame-retardance mechanism, which is described in detail elsewhere.<sup>46</sup>

**TABLE IV**  
**Fire Performance Index (FPI) of DGEBA and TGDDM Systems**

DGEBA system	FPI (sm <sup>2</sup> /kW)	TGDDM system	FPI (sm <sup>2</sup> /kW)
DGEBA only	0.046	TGDDM only	0.038
7.5% Clay–DGEBA	0.054	7.5% Clay–TGDDM	0.045
3.0% Phos–DGEBA	0.080	3.0% Phos–TGDDM	0.061
3.0% Phos–7.5% clay–DGEBA	0.049	3.0% Phos–7.5% clay–TGDDM	0.053

Similar results were found in the case of the TGDDM system. The peak rate of heat release for unmodified TGDDM was about 1304 kW/m<sup>2</sup>. When TGDDM was modified with 7.5% clay, a lower peak rate of release of 1090 kW/m<sup>2</sup> occurred, some 17% less. Similar to DGEBA, TGDDM modified with 3% phosphorus showed a peak release rate at 637 kW/m<sup>2</sup>, some 52% lower than that of unmodified TGDDM. TGDDM modified with both phosphorus and clay has a peak heat release rate at 682 kW/m<sup>2</sup>, 48% lower than that of unmodified TGDDM. Similar to the DGEBA system, on the addition of both phosphorus and clay in TGDDM, no synergistic effect on RHR was observed. Other important parameters obtained from the epoxy and modified epoxies by cone calorimetry are given in Table III.

Evaluation of fire performance of epoxy resins involves quantifying smoke generation at a specific extinction area (SEA) and quantifies production of CO and CO<sub>2</sub>. SEA measures the total obscuration area of smoke produced, divided by the total mass loss during burn, thus measuring the efficiency of a given mass of flammable volatiles that is converted when it burns.<sup>47</sup> Figure 12(a) and (b) show the SEA of DGEBA or TGDDM and modified DGEBA/TGDDM as a function of time. The SEA value of phosphorus–DGEBA and phosphorus–clay–DGEBA in Figure 12(a) was found to be higher and occurred for a longer time compared to DGEBA. This can be explained by the fact that phosphorus–DGEBA system converted into smoke more easily when it burns and does so over a longer period of time. CO<sub>2</sub> emission during burning show in Figure 13(a) and (b) that the CO<sub>2</sub> rate is always higher for the DGEBA or TGDDM system and clay–DGEBA or TGDDM compared to phosphorus–DGEBA or TGDDM and clay–phosphorus–DGEBA or TGDDM epoxy resins system. The result indicates that during the burning process, DGEBA or TGDDM and clay-modified DGEBA or TGDDM are completely condensed. This is supported by the lower production level of CO of DGEBA/TGDDM and clay-modified DGEBA/TGDDM, as shown in Figure 14(a) and (b). Higher CO production of DGEBA or TGDDM and clay-modified DGEBA or TGDDM indicates incomplete combustion and possibly the gas-phase activity. Clay-modified DGEBA or TGDDM in Figure 12(a) and (b) showed lower SEA values compared to those of

phosphorus or both phosphorus–clay-modified DGEBA or TGDDM. Thus the synergistic effect of clay and phosphorus in DGEBA or TGDDM system was not observed.

The total fire performance of a material can also be understood from the fire performance index (FPI), which is the ratio between the time of ignition (time) and the peak rate heat release (RHR). Table IV shows the FPI of DGEBA or TGDDM and modified DGEBA or modified TGDDM. DGEBA or TGDDM without any modification show the lowest fire performance at 0.046 and 0.038 sm<sup>2</sup>/kW, respectively. However, when DGEBA and TGDDM are modified with phosphorus the FPI increased to 0.080 for the DGEBA system, an increase of 74%; comparatively, the phosphorus-modified TGDDM improved 61%. Improvement in fire performance was also observed by incorporation of clay into both DGEBA and TGDDM systems as shown in Table IV. Unfortunately, however, the modification of epoxy by the addition of both clay and phosphorus on FPI showed no synergistic effect. FPI values (i.e., fire performance of epoxy) could potentially have been greater in either the clay- or phosphorus-modified system if the unexpected reduction of time of ignition had not occurred earlier (lower time of ignition), as shown in Table III. A lower time to ignition in the phosphorus-modified system might be attributable to initial combustion of phosphorus moiety before these could perform as fire retardants. The decrease in time to ignition was also observed in the modified polypropylene system by Gallina et al.,<sup>48</sup> who suggested that this was attributed to early combustion of fire-retardant materials before they play their own role in the material during firing. Other properties of materials, mainly the mechanical properties before and after firing tests of the composites, should be investigated further.

## CONCLUSIONS

In this work, we synthesized organo-phosphorus epoxy of DGEBA and TGDDM and investigated their chemical, thermal, and fire performance properties. We also fabricated clay-based nanocomposites and phosphorus-containing epoxy resins of two different functionalities to investigate the possibility of synergistic effects of clay and phosphorus on thermal and

flame properties. We also investigated the flammability of DDGEBA or TGDDM-phosphorus epoxy and blend of phosphorus-clay and epoxy by cone calorimeter. Among the additives epoxy modified by organophosphorus compound or clay-modified epoxy showed significantly improvement in fire retardance. Modification of the epoxy resin by incorporating both clay and phosphorus compound showed no synergistic improvement on fire-performance property.

## References

1. Cheng, K. C.; Lai, K. C.; Chiu, W. J. *J Appl Polym Sci* 1999, 71, 721.
2. May, C. A. *Epoxy Resins: Chemistry and Technology*, 2nd ed.; Marcel Dekker: New York, 1988.
3. Lee, H.; Nevellie, K. *Hand Book of Epoxy Resin*; McGraw-Hill: New York, 1967.
4. Wong, C. P. *Adv Polym Sci* 1988, 84, 63.
5. Cheng, K. C. *J Polym Sci Polym Phys Ed* 1998, 36, 2339.
6. Gamino, G.; Costa, L.; Martinasso, G. *Polym Degrad Stab* 1989, 18, 227.
7. Yamazaki, K. H.; Hori, T. U.S. Pat. 5,096,980, 1992.
8. Maiti, S.; Banerjee, S.; Palit, S. K. *Prog Polym Sci* 1993, 18, 227.
9. Liu, Y. L.; Hsuie, G. H.; Lee, R. H.; Chiu, Y. S. *J Polym Sci Part A: Polym Chem* 1997, 35, 565.
10. Liu, Y. L.; Hsuie, G. H.; Lee, R. H.; Chiu, Y. S. *J Appl Polym Sci* 1997, 63, 895.
11. Wang, C. S.; Lin, C. H. *J Appl Polym Sci* 1999, 74, 1635.
12. Derouet, D.; Morvan, F.; Brosse, J. C. *J Appl Polym Sci* 1996, 62, 1855.
13. Buckingham, M. R.; Lindsay, A. J.; Stevenson, D. E.; Muller, G.; Morel, E.; Costes, B.; Henry, Y. *Polym Degrad Stab* 1996, 54, 311.
14. Cheng, K.-C.; Yu, S.-Y.; Chiu, W.-Y. *J Appl Polym Sci* 2002, 83, 2741.
15. Shu, W.-J.; Yang, B.-Y.; Chin, W.-J.; Perng, L.-H. *J Appl Polym Sci* 2002, 84, 2080.
16. Wang, C. S.; Sheigh, J. Y. *Polymer* 1998, 39, 5819.
17. Hussain, M.; Varley, R.; Mathys, Z.; Simon, G. P. *J Appl Polym Sci*, to appear.
18. Giannelis, E. P.; Krisnamoorti, R. K.; Manias, E. *Adv Polym Sci* 1998, 138, 107.
19. Alexandre, M.; Dubois, P. *Mater Sci Eng Rep* 2000, 28, 1.
20. Gilman, J. W.; Jackson, C. L.; Morgan, A. B.; Harris, R.; Manias, E.; Giannelis, E. P.; Wuthenow, M.; Hilton, D.; Phillips, S. H. *Chem Mater* 2000, 12, 1866.
21. Gilman, J. W.; Kashiwagi, T.; Lomakin, S.; Jones, P.; Lichtenham, J.; Giannelis, E. P.; Manias, E. *Proc Int Wire Cable Symp* 1998, 46, 761.
22. Gilman, J. W.; Kashiwagi, T.; Giannelis, E. P.; Manias, E.; Lomakin, S.; Lichtenham, J.; Jones, P. *Chemistry and Technology of Polymer Additives*; Blackwell Science: Oxford, UK, 1999; Chapter 14, p. 249.
23. Lin, C. H.; Wang, C. S. *Polymer* 2001, 42, 1869.
24. Gilman, J. W.; Kashiwagi, T.; Lomakin, S.; Jones, P.; Lichtenham, J.; Giannelis, E. P.; Manias, E. *SAMPE Symp* 1998, 43, 1053.
25. Wang, C. S.; Lin, C. H. *J Polym Sci Part A: Polym Chem* 1999, 37, 3903.
26. Hou, S. S.; Chung, Y. P.; Chan, C. K.; Kuo, P. L. *Polymer* 2000, 41, 3263.
27. ASTM E1354-92. *Annu Book ASTM Stand* 1992.
28. Musto, P. P.; Mascia, L.; Ragosta, G.; Scaramizi, G.; Villao, V. *Polymer* 2000, 41, 565.
29. Lan, T.; Pinnavaia, T. J. *Chem Mater* 1994, 6, 2216.
30. Jiankun, L.; Yucai, K.; Zongneng, Q.; Xiao-Su, Y. *J Polym Sci Part B: Polym Phys* 2001, 39, 115.
31. Brown, J. M.; Curliss, D.; Vaia, R. A. *Chem Mater* 2000, 12, 3376.
32. Wang, C. S.; Yeh, J. F.; Shau, M. D. *J Appl Polym Sci* 1996, 59, 215.
33. Becker, O. M.S. Thesis, Monash University, Clayton, Australia, 2001.
34. Lan, T.; Kaviratna, P. D.; Pinnavaia, T. J. *J Phys Chem Solids* 1996, 57, 1005.
35. Kornmann, X.; Lindberg, H.; Berglund, L. A. *Polymer* 2001, 42, 1303.
36. Liu, Y. L.; Hsuie, G. H.; Lee, R. H.; Chiu, Y. S.; Jeng, R. J.; Perng, L. H. *J Appl Polym Sci* 1996, 61, 613.
37. Liaw, D. J. *J Polym Sci* 1997, 35, 2365.
38. Pogany, G. A. *Polymer* 1970, 11, 66.
39. Kelly, P.; Akelah, A.; Qutubuddin, S.; Moet, A. *J Mater Sci* 1994, 29, 2274.
40. Musto, P.; Ragosta, G.; Russo, P.; Mascia, L. *Macromol Chem Phys* 2001, 202, 3445.
41. Massam, J.; Pinnavaia, T. J. In: *Clay Nanolayer Reinforcement of a Glassy Epoxy Polymer*, Proceedings of the Materials Research Society Symposium, 1998.
42. Lee, A.; Lichtenhan, J. D. *J Appl Polym Sci* 1999, 73, 1993.
43. Kornmann, X.; Thmann, R.; Mulhaupt, R.; Finter, J.; Berglund, L. A. In: *proceedings of the NRCC/IMI International Symposium on Polymer Nanocomposites Science and Technology*, Polymer Nanocomposites 2001, Montreal Canada, 2001.
44. Becker, O.; Varley, R. J.; Simon, G. P. *Polymer* 2001, 43, 4365.
45. Jeng, R. J.; Shau, S. M.; Lin, J. J.; Su, W. C.; Chiu, Y. S. *Eur Polym J* 2002, 38, 683.
46. Ebdon, J. R.; Hunt, B. J.; Joseph, P.; Konkel, C. S.; Price, D.; Pyrah, K.; et al. *Polym Degrad Stab* 2000, 70, 425.
47. Whiteley, R. H. *Fire Mater* 1994, 18, 57.
48. Gallina, G.; Bravin, E.; Badalucco, C.; Audisio, G.; Armanini, M.; Chirico, A. D.; Provasoli, F. *Fire Mater* 1998, 22, 15.